Holz als Roh- und Werkstoff (2006) 64: 125–133
DOI 10.1007/s00107-005-0032-5

ORIGINALARBEITEN · ORIGINALS

Heiko Thoemen · Clovis R. Haselein · Philip E. Humphrey

Modeling the physical processes relevant during hot pressing of wood-based composites. Part II. Rheology

Published online: 28 September 2005

Abstract A rheological model to describe the development of the vertical density profile and of internal stresses within wood-furnish mats during hot pressing is presented in this paper. The rheological model is part of a comprehensive three-dimensional simulation model that accounts for those mechanisms most important during the pressing process, including heat and mass transfer inside the mat and adhesive cure.

To model the rheological behavior of the mat, the four-element Burgers model commonly used to describe visco-elastic material behavior has been expanded with the addition of a fifth element that represents plastic and micro-fracture related deformation. The coefficients of the non-linear model are highly dependent on the material conditions. Equations of the coefficients as a function of temperature, moisture content and density, as well as a mathematical formulation of the five-element model is presented in this paper. Furthermore, model predictions for both a batch and a continuous press are given. A comparison with experimental results shows that the expanded Burgers model is suitable to predict typical features of the vertical density profile, such as the development of density maxima near the surfaces, shoulders or side maxima as a consequence of intermediate or final densification steps, and differences in the density profile between the mat center and the edges in the horizontal plane. Such agreement provides the basis for a wide range of industrial and research applications.

Modellierung der physikalischen Vorgänge beim Heißpressen von Holzwerkstoffen. Teil 2. Rheologie

Zusammenfassung Im vorliegenden Artikel wird ein rheologisches Modell zur Beschreibung der Entwicklung des Dichteprofils senkrecht zur Plattenebene sowie der Spannungen innerhalb des Holzwerkstoffvlieses während des Heißpressens vorgestellt. Das rheologische Modell ist Bestandteil eines umfassenden drei-dimensionalen Simulationsmodells, welches weitere für den Pressvorgang wichtige Vorgänge wie Wärme- und Stofftransport und Klebharzaushärtung beinhaltet.

Zur Modellierung des rheologischen Vliesverhaltens wurde das aus vier Elementen bestehende Burgers-Modell, das sich zur Beschreibung von visko-elastischen Verformungen eignet, um ein fünftes Element für plastische und microbruchinduzierte Verformungen ergänzt. Die Koeffizienten des nicht-linearen Modells hängen in starkem Maße vom Vlieszustand ab. Gleichungen zur Beschreibung der Koeffizienten als Funktion von Temperatur, Feuchte und Dichte werden zusammen mit der mathematischen Formulierung des Fünf-Elemente-Modells präsentiert. Darüber hinaus werden Modellrechnungen sowohl für Takt- als auch für Doppelbandpressen dargestellt. Ein Vergleich mit experimentellen Ergebnissen zeigt, dass das erweiterte Burgers-Modell für die Vorhersage der charakteristischen Merkmale eines Dichteprofils geeignet ist; charakteristisch sind die Entwicklung von oberflächennahen Dichtemaxima, von Schultern oder Zwischenmaxima als Folge von Zwischen- oder Nachverdichtungsschritten sowie Unterschiede im Dichteprofil zwischen der horizontalen Mattenmitte und den Kanten. Die gute Übereinstimmung zwischen Simulation und Experiment bietet die Grundlage für den Einsatz des Simulationsmodells für eine Reihe von Anwendungen in Industrie und Forschung.

H. Thoemen (✉)
Department of Wood Science, University of Hamburg,
Leuschnerstrasse 91, 21031 Hamburg, Germany
E-mail: thoemen@holz.uni-hamburg.de

C.R. Haselein
Universidade Federal de Santa Maria, Santa Maria, Brazil

P.E. Humphrey
Adhesive Evaluation Systems, Inc., 1235 NW Kainui Drive, Corvallis, OR 97330, USA and College of Forestry, Oregon State University, Corvallis, OR 97331-7402, USA

1 Introduction

An integrated model to simulate the hot pressing process of wood-based composites is presented in this pair of papers. Both aspects of the process, the evolution of temperature, moisture and gas pressure variations on the one hand and of density variations on the other hand, are closely linked with each other: The resistance of the wood-furnish material to an external force is, among others, a function of temperature and moisture content, while on the other hand the temperature and moisture content development is affected by density. Hence, a process model based on fundamental principles requires the simultaneous treatment of mass and heat transfer, and material densification. While the mass and heat transfer processes have been described in the first paper (Thoemen and Humphrey 2005), the densification behavior of the wood-furnish mat, the development of the cross-sectional density profile, and the build-up and relaxation of internal stresses is dealt with in the present paper.

The study of time-dependent stress-strain behavior of materials is called rheology (Bodig and Jayne 1982). Taking the term 'rheology' in its narrower sense, it describes only phenomena such as viscous or delayed-elastic deformation and stress relaxation. However, when a wood-furnish mat is consolidated in the hot press, the material experiences both time-dependent and instantaneous deformation. The term 'rheology' is used here in such a broader sense. This reflects the fact that both aspects of the material behavior are interactively linked with each other, and that they are described simultaneously by so-called rheological models.

The approach presented in this paper to model the rheological material behavior during hot pressing goes back on work done by Ren (1991) working together with Humphrey. It uses a rheological model, consisting of three springs and two dashpots. Each of the coefficients to mathematically describe the five elements is a function of temperature, moisture content and density. Humphrey (1994) merged the rheological model with a mass and heat transfer model to predict the development of the cross-sectional density profile for MDF.

A different approach has been developed by Steiner and Dai (1993), Lang and Wolcott (1996) and Lenth and Kamke (1996). The models of these three research groups have in common that the compaction behavior of the mat is assumed to be governed by two independent factors: The geometry and alignment of the wood constituents, and the properties of solid cell wall substance. Dai et al. (2000) and Zombori (2001) applied this approach for simulating the cross-sectional density profile formation. So far, such research based on probabilistic and geometrical theory to model mat consolidation has been restricted to mats made of strands or small pieces of veneer, but cannot be used for MDF.

2 Rheological behavior of wood-furnish mats

When load is applied to a loosely formed wood-furnish mat, the material experiences multiple modes of deformation. Both, the structure of the individual wood constituents and their arrangement with respect to each other change considerably during densification. Bending, compression, shear and fracture of the cell wall substance, cell collapse, and friction among the wood constituents all contribute to the net strain of the material. Only a proportion of the total strain is recoverable when the load is reduced or removed. Evidence of such strain recovery is the expansion of the mat after pre-pressing and the spring-back of the panel after hot pressing.

Mat compaction results in compressive stresses inside the wood-furnish material, and these counteract the external pressing pressure. As wood is a visco-elastic material, part of this stress will relax with time. Stress relaxation processes during pressing become evident in typical pressing pressure-versus-time curves recorded under conditions where the mat thickness is held constant after compaction without using spacing strips or stops. Early experiments under such conditions have been reported by May and Mehlhorn (1969) and Liiri (1969). The pressure-versus-time curves typically show an immediate pressure drop after the final thickness was reached, and then flatten out.

The rheological behavior of the wood-furnish material, i.e. the stress-strain relationship and its changes over time, is highly dependent on a number of factors, the most important ones being material characteristics, moisture and temperature conditions, state of adhesive curing, and the history of the material. The first three are considered in turn:

- Material characteristics include dimensions and alignment of the wood constituents, the wood species used, and the density of the raw material. The effects of such parameters on the densification behavior of mats have been investigated, for example, by Kull (1963), Kehr and Schölzel (1965), and Kavvouras (1977). These parameters may vary considerably among different furnish types, but do not (or only little) change during pressing.
- The cell wall substance of solid wood tends to soften with increasing temperature and moisture content. Similar temperature and moisture effects are well known for wood-furnish materials (e.g. Kehr and Schölzel 1965, von Haas 1998). Although such plasticisation of the material has been recognized for all temperature and moisture levels, above a critical temperature, known as the glass transition temperature, wood, like many other polymers, experiences a transition that enhances its softening effect. Temperature and moisture content clearly change with location and time during hot pressing. It was early appreciated that the variation of these two factors causes non-uniform densification, resulting in a typical cross-sectional density profile (Fahrni 1956, Kollmann 1957). Furthermore, as temperature and moisture content do also vary within the horizontal plane of the mat (or across the width of a mat in a continuous press), in-plane variations of the cross-sectional density profile can be expected. Such variations are a common problem in the industrial process.
- Once the adhesive starts to cure, inter-particle adhesive bonds develop. Part of the compressive deformation of the wood constituents becomes fixed, or 'locked', so that not the entire elastic and delayed-elastic strain components cease to be fully recoverable. As a consequence, the spring-back of the mat inside the press or of the panel when leaving the press is reduced.

3 Modeling the rheological behavior

3.1 The Burgers–Humphrey model

Rheological models are frequently used as analogies to illustrate and arithmetically describe the stress-strain relationship of materials. In such models, the strain is split into individual components, such as elastic or viscous strain. Each strain component is represented by a simple element (e.g., a spring or a dashpot) or by a combination of such elements. The elements may be characterized by theoretical properties, hereafter referred to as rheological coefficients. The rheological coefficients are typically determined experimentally, and the stress-strain relationship can be calculated once these coefficients are known.

A rheological model commonly employed to explain the deformation behavior of visco-elastic materials is the so-called Burgers model (Fig. 1a). The Burgers model is a series-connection of a Maxwell model (spring and dashpot in series) and a Kelvin model (spring and dashpot in parallel, sometimes called Voigt model); it describes a material that simultaneously experiences elastic, viscous and delayed-elastic deformation upon the application of stress. As wood shows such visco-elastic material behavior, some researchers used the Burgers model to describe creep and stress relaxation processes of solid wood under load (e.g. Kollmann 1961). The Burgers model may also be employed to calculate the creep behavior of wood-based panels in use (Pierce and Dinwoodie 1977).

One limitation of the Burgers model is, however, that it is only applicable for situations where any instantaneous deformation is elastic and, therefore, recoverable. In other words, irreversible deformation that happens instantaneously upon loading cannot be described by the Burgers model. Raczkowski (1969) pointed out that, when bending solid wood, such a type of deformation might occur due to microscopically small destruction processes in the wood. When compressing a loosely formed wood-furnish mat close to its final density level, it is even more obvious that part of the immediate deformation is not recoverable.

Ren (1991), therefore, supplemented the Burgers model by adding a plastic and micro-fracture (PMF) element. The Burgers model and the PMF element are connected in series, so that the extended Burgers model (Burgers–Humphrey model, Fig. 1b) accounts for both the visco-elastic behavior of the mat as well as irreversible changes of cell wall and mat structure that happen instantaneously upon loading. According to Ren's definition, strain due to PMF effects only occurs if the effective stresses exceed the yield strength of the microstructures; this type of strain is not recoverable when the load is removed. Such behavior may be symbolized by a spring that only operates in one direction.

As becomes obvious from Fig. 1b, there are five rheological coefficients required to characterize the rheological behavior of a material by the Burgers–Humphrey model. Such coefficients for medium density fiberboard (MDF) mats will be presented below.

Figure 2 shows the response of each of the four strain components represented by the Burgers–Humphrey model when applying a sudden stress at time t_0, then keeping the stress constant for a certain period until t_1, and eventually dropping the stress to zero again. As can be seen from this figure, elastic as well as PMF deformation occurs instantaneously upon the application of stress, whereas viscous and delayed-elastic deformations are time-dependent. Further, it should be noticed that only elastic and delayed-elastic deformation are recoverable after the stress is removed at t_1, but not the other two strain components. A sche-

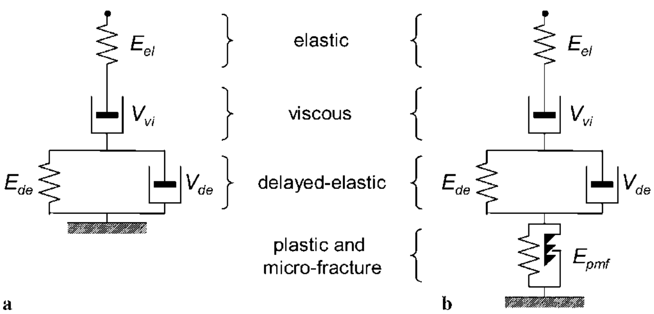

Fig. 1 a Burgers model. **b** Five-element Burgers–Humphrey model, representing four strain components. Refined after Ren (1991). E = modulus of elasticity, V = viscosity, E_{pmf} = coefficient for plastic and micro-fracture element. The non-linear behavior of each element is not symbolized in this schematic

Abb. 1 a Burgers-Modell. **b** Burgers-Humphrey-Modell mit fünf Elementen zur Beschreibung von vier Verformungskomponenten. In Anlehnung an Ren (1991). E = Elastizitätsmodul, V = Viskosität, E_{pmf} = Koeffizient für plastische und microbruchinduzierte Verformungen. Das nicht-linare Verhalten der einzelnen Elemente ist hier nicht dargestellt

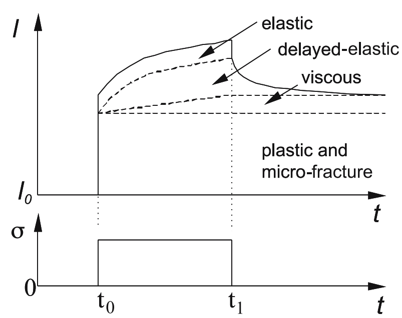

Fig. 2 The four strain components described by the Burgers–Humphrey model as a function of stress σ and time t

Abb. 2 Vier Verformungskomponenten des Burgers-Humphrey-Modells als Funktion von Spannung σ und Zeit t

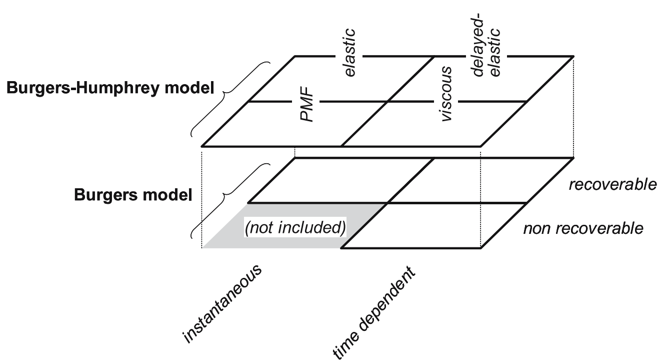

Fig. 3 The three strain components of the Burgers model and the four strain components of the Burgers–Humphrey model, categorized according to different types of deformation. PMF = plastic and micro-fracture

Abb. 3 Drei Verformungskomponenten des Burgers-Modells und vier Verformungskomponenten des Burgers-Humphrey-Modells, angeordnet nach Verformungsarten. PMF = Plastische und microbruchinduzierte Verformung matic defining the different types of deformation is displayed in Fig. 3.

3.2 Further model assumptions

The non-linear Burgers–Humphrey model as it is presented above is used in this work to describe the stress-strain relationship of the wood-furnish mat during hot pressing. Only normal compressive stresses acting perpendicular to the mat plane are considered. No shearing stresses are assumed, so that horizontal coupling between regions is not accounted for. Due to the lack of reliable Poisson's ratio values for wood-furnish materials in the literature, and to maintain the simplicity of a one-dimensional rheological model, lateral spreading of the mat is ignored. Noticeable lateral spreading can be expected at the early stages of press closure when the mat is relatively loose. Furthermore, lateral spreading may lead to slight density reductions near the edges of the mat. However, these effects are unlikely to have a significant impact on overall simulation results.

The impact of adhesive cure on the rheological mat behavior is not accounted for in the present approach. This simplification will certainly affect the predictions of events, such as stress relaxation processes, strain recovery upon press opening, and slight shifting processes of the density profile at later stages of the pressing cycle. On the other hand, the compressibility of the material is believed to be only little affected by the state of adhesive curing.

3.3 Mathematical formulation

The Burgers–Humphrey model accounts for four different sources of deformation (Fig. 1b). These are elastic (el), viscous (vi), delayed-elastic (de), and plastic and micro-fracture (pmf) strain. The total local strain $\Delta\varepsilon$ during a short time step Δt is the sum of these four strain components:

$$\Delta\varepsilon = \Delta\varepsilon_{\mathrm{el}} + \Delta\varepsilon_{\mathrm{vi}} + \Delta\varepsilon_{\mathrm{de}} + \Delta\varepsilon_{\mathrm{pmf}} \tag{1}$$

with $\Delta\varepsilon$ being the 'true strain', which is defined as

$$\Delta\varepsilon = -\frac{l_2 - l_1}{l_1} \tag{2}$$

For convenience, the sign convention is chosen so that compressing the layer yields a positive strain.

To apply the Burgers–Humphrey model to the hot pressing process, an appropriate mathematical formulation is needed. Expressions will be listed here in turn for each of the four strain components. A presentation of derivations is beyond the scope of this paper; they can be found in Thoemen (2000).

The elastic strain component, $\Delta\varepsilon_{\mathrm{el}}$, represented by the simple spring in Fig. 1b, may be calculated as:

$$\Delta\varepsilon_{\mathrm{el}} = \frac{1}{E_{\mathrm{el}}}\Delta\sigma - \frac{\sigma}{E_{\mathrm{el}}^2}\Delta E_{\mathrm{el}} \tag{3}$$

where σ is the stress acting perpendicular to the mat plane, and E_{el} is the modulus of elasticity of the elastic element. Both quantities are given in the units of Pa. In this equation the second term on the right hand side acknowledges the assumption that instantaneous deformations are caused not only by a change of σ, but also by a change of E_{el}.

The viscous material behavior is described by a single dashpot. This strain component, $\Delta\varepsilon_{\mathrm{vi}}$, that emerges during the small time interval Δt [s] is proportional to the prevailing stress σ [Pa], and is inverse proportional to the viscosity V_{vi} [Pa s]:

$$\Delta\varepsilon_{\mathrm{vi}} = \frac{\sigma}{V_{\mathrm{vi}}}\Delta t \tag{4}$$

It becomes clear from Eq. 2 that a sudden change of σ or V_{vi} does not lead to an instantaneous deformation of the viscous element.

The delayed-elastic component of the material behavior, $\Delta\varepsilon_{\mathrm{de}}$, is symbolized by the Kelvin model. The strain $\Delta\varepsilon_{\mathrm{de}}$ at time t for the Kelvin model can be calculated by:

$$\Delta\varepsilon_{\mathrm{de}} = \frac{(\sigma - \sigma_s)}{V_{\mathrm{de}}}\Delta t \tag{5}$$

with:

$$\sigma_s = \sum_0^t \Delta\sigma_s = \sum_0^t \left(\frac{E_{\mathrm{de}}(\sigma - \sigma_s)}{V_{\mathrm{de}}}\Delta t + \frac{\sigma_s}{E_{\mathrm{de}}}\Delta E_{\mathrm{de}}\right) \tag{6}$$

E_{de} and V_{de} denote the rheological coefficients for the spring and the dashpot, respectively, of the Kelvin model. The total stress σ is the sum of the stress components acting on the spring, σ_{s}, and on the dashpot, $\sigma - \sigma_{\mathrm{s}}$. Unlike the single spring and dashpot, the strain represented by a Kelvin model does not only depend on the prevailing values of the effective stress and rheological coefficients, but also on the previous course of deformation.

Strain as a consequence of plastic and micro-fracture (PMF) effects is represented by a spring that experiences compression upon application of load, but that stays in its position of maximum compression when the load is partially or fully removed.

Let us define c_{crit} as a constant that stores the conditions of the last time the effective stress σ exceeded the yield strength σ_{yield}. The following set of equations provides a mathematical formulation of the PMF element:

$$\sigma_{\mathrm{yield}} = c_{\mathrm{crit}} \cdot E_{\mathrm{pmf}} \tag{7}$$

$$\text{if: } \sigma > \sigma_{\mathrm{yield}} : \Delta\varepsilon_{\mathrm{pmf}} = \frac{1}{E_{\mathrm{pmf}}}\Delta\sigma - \frac{\sigma}{E_{\mathrm{pmf}}^2}\Delta E_{\mathrm{pmf}}\,; \quad c_{\mathrm{crit}} = \frac{\sigma}{E_{\mathrm{pmf}}} \tag{8}$$

$$\text{if: } \sigma \le \sigma_{\mathrm{yield}} : \Delta\varepsilon_{\mathrm{pmf}} = 0; \qquad c_{\mathrm{crit}} = \text{const} \tag{9}$$

where E_{pmf} denotes the coefficient of the plastic and micro-fracture strain component. Further deformation may only happen if the effective stress σ surpasses the yield strength of the material, σ_{yield}. In this case, the constant c_{crit} has to be updated to store the new criterion for the yield strength.

3.4 Boundary conditions

In the present paper the boundary conditions relevant to modeling rheological mat behavior will be described for the batch press, while a description of the model boundaries for the continuous press has been presented in Thoemen and Humphrey (2003).

The model presented here can be operated in either position control and load control mode, or in a combination of both. The final thickness of the mat is assumed to not be dictated by spacing strips mounted on the pressing platens, or by similar devices.

In the case of position control, the target thickness of the mat is specified for distinct times, and the thickness values for any intermediate time can be obtained by linear interpolation between the two adjacent thickness values specified. The pressing platens are assumed to be rigid, forcing the mat to have a constant thickness d across its x–y plane.

When the modelled press is operated in load control mode, the pressing pressure is specified in a similar way to that for thickness. It is assumed that the applied stress is the same all over the x–y plane. Consequently, the thickness response may alter with position in the x–y plane due to different temperature and moisture conditions, implying that the pressing platens are not rigid but are allowed to bend.

3.5 Coefficients of the Burgers–Humphrey model

Five rheological coefficients, i.e. one for each element of the Burgers–Humphrey model, are needed to describe the stress-strain relationship of the material. These coefficients are functions of temperature, moisture content and density, and may be determined by recording and evaluating the strain response to a defined stress course in a miniature sealed press system.

Two different sets of data are available so far, either of which may be used for the simulation model. The first one was measured by Ren (1991) and fitted to equations by Haselein (1998). The second set of data was obtained by von Haas (1998) for MDF fiber, particle and strand materials. Von Haas's data for MDF fiber will be used for those simulation runs discussed in this paper.

von Haas (1998) described the mat behavior separately for different states of the pressing process; he did not explicitly use the Burgers–Humphrey model, which integrates the most important aspects of the material behavior into one approach. The five rheological coefficients of the Burgers–Humphrey model can, however, be derived from the results of two different experiments reported by von Haas. Only the final equations to calculate the coefficients are presented here, while derivations are described in more detail by von Haas (1998) and by Thoemen (2000). The four rheological coefficients for elastic, viscous and delayed-elastic deformation may be computed as

$$\ln C = a_1 u + b_1 T + c_1 + \rho\, e^{(a_2 u + b_2 T + c_2)} - \ln\left(\frac{\rho}{198.3}\right) \qquad (10)$$

where C represents the rheological coefficients E_{el}, V_{vi}, E_{de} and V_{de}. The constants a, b and c are presented in Table 1. Temperature T, moisture content u and material density ρ are in the units of °C, % and kg m^{-3}, respectively. An expression for the remaining coefficient, E_{pmf}, is given by

$$\ln E_{\text{pmf}} = 17.10 - \frac{88.44}{\ln \rho} - 7.57 \times 10^{-2} u - 8.53 \times 10^{-3} T \qquad (11)$$

where E_{pmf} is in the units of MPa.

4 Model predictions

4.1 Batch press simulation

Model predictions of the rheological mat behavior and of the cross-sectional density profile development in a batch press are presented here and compared to experimental data. The input parameters for the simulation runs have been chosen according to the conditions for MDF mats that have been pressed in a large-size (4 × 8 ft.) laboratory hot press to a target thickness and density of 39 mm and 697 kg m^3, respectively. Experimental set-up, initial and boundary conditions for the simulation runs, as well as model predictions of mat temperature, gas pressure and moisture content development of the same simulations are described in Thoemen and Humphrey (2005). A total of four trials were carried out in the experiment, with the pressing schedule being the only parameter varied among the four trials; as trial 4 was a repetition of trial 3, only trials 1 to 3 are referred to in this paper. In trial 1 the press was closed to final thickness in only one densification step, whereas a second densification step at a later stage of the pressing cycle was included in the other trials. No spacing strips or similar devices have been used in the experiments.

Table 1 Constants presented by von Haas (1998) for Eq. 10 to calculate the rheological coefficients for MDF mats

Tabelle 1 Konstanten nach von Haas (1998) zur Berechnung der rheologischen Koeffizienten für MDF-Vliese

	a_1	b_1	c_1	a_2	b_2	c_2
E_{el}[MPa]	4.22×10^{-2}	-2.74×10^{-2}	$3.25 \times 10^{+0}$	-1.86×10^{-2}	3.24×10^{-3}	$-5.10 \times 10^{+0}$
V_{vi}[MPa s]	-3.87×10^{-2}	-2.09×10^{-2}	$9.71 \times 10^{+0}$	-2.45×10^{-2}	2.22×10^{-3}	$-5.32 \times 10^{+0}$
E_{de}[MPa]	-1.57×10^{-2}	-2.37×10^{-2}	$3.70 \times 10^{+0}$	-2.17×10^{-2}	3.11×10^{-3}	$-5.33 \times 10^{+0}$
V_{de}[MPa s]	-1.24×10^{-1}	1.30×10^{-3}	$5.29 \times 10^{+0}$	2.45×10^{-2}	-2.23×10^{-3}	$-5.34 \times 10^{+0}$

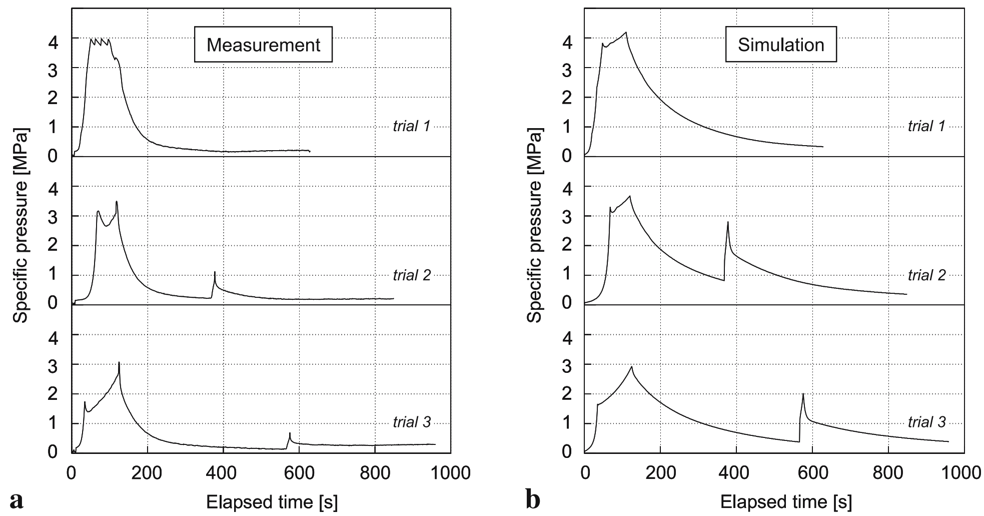

Fig. 4 Comparison of recorded (**a**) and predicted (**b**) pressing pressure. Displayed are curves for batch press trials 1 to 3

Abb. 4 Vergleich von gemessenem (**a**) und vorhergesagtem (**b**) Pressdruck. Dargestellt sind Kurven für die Versuche 1 bis 3, Taktpresse

4.1.1 Pressing pressure

A comparison of recorded and simulated pressing pressure courses is displayed in Fig. 4. All curves show the typical course of pressure buildup during press closure, and the subsequent decline of the pressing pressure, due to stress relaxation processes, while keeping the thickness of the mat constant. Except for the measured pressure in trial 1 where the maximum pressure was limited by the press hydraulics, the measured and predicted curves show pressure peaks that coincide with the changes in the consolidation rate. The late pressure maxima in trials 2 and 3 are caused by the second densification steps to final mat thickness introduced in these pilot plant trials.

Although stress relaxation is somewhat underestimated in the simulations, overall there is good qualitative and quantitative agreement between experimental data and model predictions. Inaccuracies in model predictions during the later stage of the pressing cycle are possibly due to small differences between that fiber material employed when determining the rheological coefficients and that one used in the experiment. Above, the coefficients have been measured for un-resinated material, while, in the experiment, a urea-formaldehyde resin was applied to the fibers and the mats were formed several hours before they were pressed.

4.1.2 Cross-sectional density profile

Due to the significant influence that cross-sectional density profiles have on many panel properties, its formation throughout the pressing cycle has been of considerable interest in the past. While the density profile of the final panel can be measured, little is known about time dependent changes in layer density during pressing. Most discussion has been rather speculative in nature so far, as there were no reliable data available. One rare source of information on the development of the density profile has been provided by Winistorfer and his co-workers (Wang et al. 2000). They developed an in-situ density monitoring system that, for the first time, allows one to measure changes in layer density during pressing. The laboratory-based system uses radiation from caesium137 sources to beam through the mat at three cross-sectional positions while the mat is consolidated in the press. Reported measurements indicate that the cross-sectional density profile is formed from a combination of actions that occur both during consolidation and also after the press has reached final position, i.e. that the density profile continues to change after press closure.

Similar conclusions can be drawn from the simulation results displayed in Fig. 5 for trial 1. During the early stages of press closure, that is before major temperature and moisture changes take place in the mat, an almost uniform densification of the entire mat is evident. Between about 50 and 110 seconds the pressing pressure persists at a high level (see Fig. 4) while the mat is compressed to its final thickness. A more or less rapid density rise in the outer mat layers is visible during this period, while the inner layers, which experience almost no temperature and moisture content changes at the early stages of pressing, show

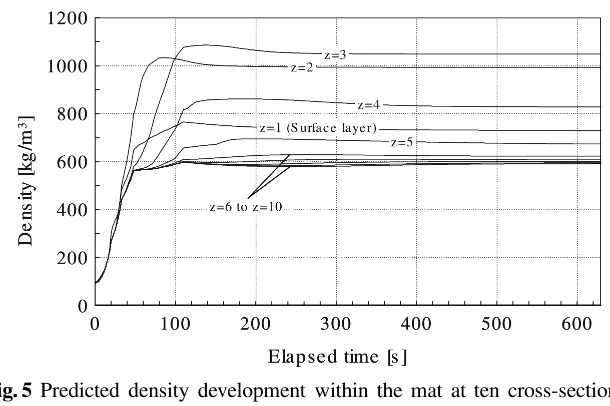

Fig. 5 Predicted density development within the mat at ten cross-sectional positions in the horizontal center. (Batch press trial 1)

Abb. 5 Vorhergesagte Entwicklung der Materialdichte an 10 über den Querschnitt verteilten Positionen in horizontaler Mattenmitte. (Versuch 1, Taktpresse)

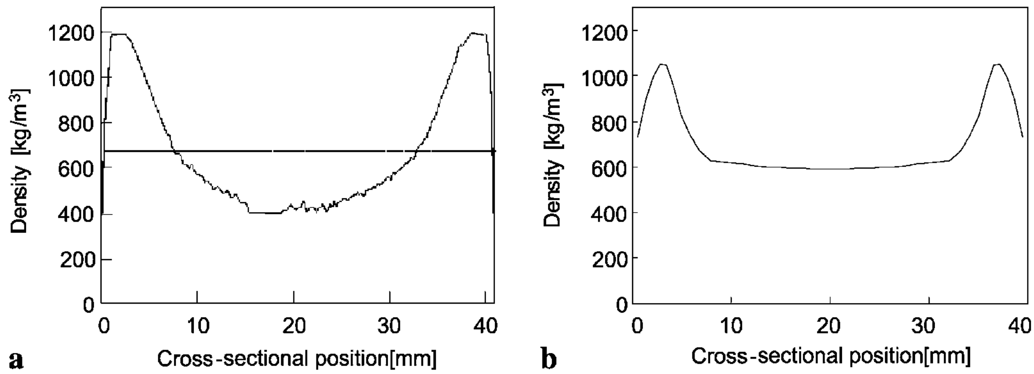

Fig. 6 Comparison of cross-sectional density profile in the horizontal center of the panel: **a** measured, **b** predicted after 630 seconds of pressing, but before press opening (Batch press trial 1)
Abb. 6 Vergleich des Dichteprofils in horizontaler Plattenmitte: **a** gemessen, **b** vorhergesagt nach 630 Sekunden Presszeit vor Pressenöffnung (Versuch 1, Taktpresse)

only a small increase in density; this is mainly caused by the viscous and delayed-elastic material behavior.

Once the final thickness has been reached at $t = 110$ s, further cross-sectional redistribution of the wood-furnish material takes place, due to proceeding changes of the rheological material properties as well as visco-elastic effects. The density in some layers continues to rise while it decreases in other layers. Most of these changes happen within the next 90 seconds, and only minor changes in layer density are predicted for the rest of the pressing cycle after $t = 200$ s. It should be noticed that the density curves displayed in Fig. 5 denote the density values on a dry wood basis. Thus, the average density of the entire mat stays constant after press closure, regardless of changes in moisture content.

The cross-sectional density profile develops as a consequence of the unequal density progressions in the different mat layers. The profile predicted here shows the typical M-shape with density maxima somewhat away from the surfaces (Fig. 6b). The pronounced density drop from the maxima towards the surfaces has been subject to some discussion in the past. The simulation results presented here demonstrate that the drop in surface density can be explained conclusively without taking into account the adhesive cure. The stiffening effect of drying counteracts the softening effect of heating in the surface layers, so that the resulting compressibility is lower than in intermediate layers. This explanation, however, does not exclude the possibility of adhesive cure having some additional impact on the density profile development, as has been proposed by some researchers (e.g. Plath 1971, Boehme 1992).

A comparison of simulated and measured final density profile is presented in Fig. 6. In both cases the profile has its maxima about 3 mm inside from the surfaces, with a steep density drop towards both the surfaces and the core. The maxima of the measured density profile are abnormally high, reaching 1240 kg/m^3, while the core density drops down to almost 400 kg/m^3. Such extreme profiles are usually not produced in industrial processes. It should be noted that even the predicted profile with maxima around 1040 kg/m^3 has to be considered as extreme, although to a less pronounced extent. Again, differences between the material property input data used for the simulation and the material characteristics of those mats used in the validation experiments may be one reason for this discrepancy.

4.2 Continuous press simulation

The simulated development of the density profile in a 28 meter long continuous MDF press is displayed in Fig. 7. Initial and boundary conditions were chosen to correspond with the industrial press used by Steffen et al. (1999) to make temperature and gas pressure measurements during pressing; they are summarized in Thoemen and Humphrey (2003).

As described for the batch press simulation above, the predicted density profile shows the typical M-shape. While those layers of maximum density close to the surfaces develop relatively early in the process, the core region experiences a considerable rise in density during the second densification step. It is the interaction between local temperature and moisture conditions on the one hand, and the course of pressing pressure on the other hand that dictate the development of the density profile. Figure 8a shows the final density profile measured for the center of the panel. The profile does not show a smooth transition from the surface to the core, but rather shoulder-shaped distortions about 4 mm inside from the surfaces. Shoulders or side maxima may develop when a pressing schedule is applied that includes two or more distinct densification steps; such effects have been described by Wang et al. (2000) for MDF pressing.

In trend, similar shoulders are predicted for the panel center, as shown in Fig. 8b. The impact of the second densification

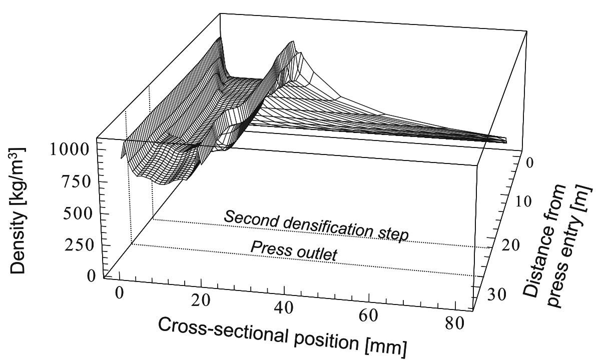

Fig. 7 Predicted density profile development within the central x–z plane of the mat (Continuous press standard run)
Abb. 7 Vorhergesagte Entwicklung des Dichteprofils entlang der mittleren x–z-Ebene des Vlieses (Standardsituation Doppelbandpresse)

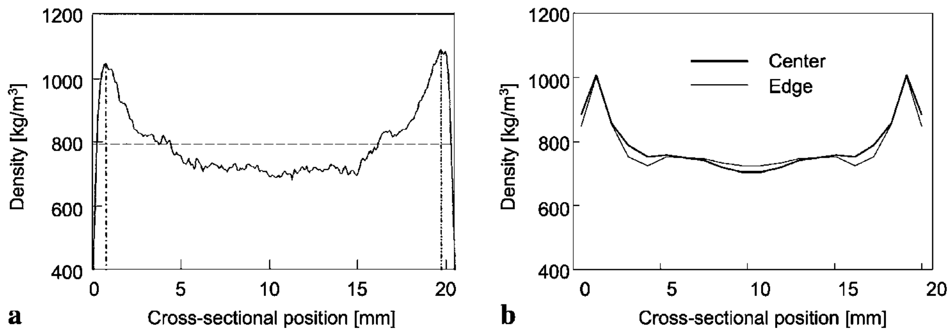

Fig. 8 Final cross-sectional density profiles. **a** Measurement for the horizontal center of the panel. **b** Predictions for the horizontal center and the position 5% inside from the edges. (Continuous press standard run)

Abb. 8 Endgültige Dichteprofile. **a** Messung für Plattenmitte. **b** Vorhersage für Plattenmitte und für die Position 5% neben der Kante (Standardsituation Doppelbandpresse)

step on the shape of the final density profile becomes clear when looking at Fig. 7. Additional test runs of the simulation program suggest that the cross-sectional density distributions are very sensitive to changes in the magnitude and course of the second densification step.

Temperature, moisture content, and consequently also rheological material properties develop somewhat differently throughout the horizontal plane of the mat. Thus, final cross-sectional density profiles vary slightly with horizontal position as is shown in Fig. 8b.

5 Conclusions

The rheological behavior of the wood-furnish mat and the development of the vertical density profile during pressing has been disputed almost since the onset of particleboard production more than half a century ago. However, during the 1970s and 80s these questions gained importance with two significant developments. The first one was the occurrence of the continuous pressing technology that prohibits the use of spacing strips and enables one to employ flexible pressing programs. The second development was the introduction of MDF into the market. More than for particleboard and OSB, the density profile is one of the most critical properties for MDF.

While almost all investigations on the density profile development and the rheological mat behavior have been rather experimental in nature until some years ago, modeling and simulating these phenomena have become a promising approach in recent years. Experiments, performed either in the industry or in the laboratory, are limited to observing interrelations between material and process parameters and final density profile. In contrast, the modeling approach also allows one to directly infer causalities. This advantage, together with the fact that simulations are by far less costly than experiments, is what makes the modeling approach valuable for research and development.

As has been demonstrated in this paper, the Burgers–Humphrey model is suitable to account for typical features of the vertical density profile. Among these are the density drop from the maxima towards the surfaces, shoulders or side maxima as a consequence of intermediate or final densification steps, and differences in density profile between mat center and edges in the horizontal plane. The rheological model used here consists of only five elements and can still be considered as relatively simple in its structure. Although the clear advantage of a straightforward model is its universal applicability and good interpretability, the addition of further elements may become necessary in the future, for example, if adhesive cure effects on the rheological mat characteristics shall be accounted for. Nevertheless, even the predictions based on the five-element model as they are presented in this paper are in good agreement, qualitatively and quantitatively, with the experimental results. Such agreement provides the basis for a wide range of applications in industry and research, including process optimization, machine design, product development and training.

Acknowledgement The authors are grateful to G. Siempelkamp GmbH & Co. for facilitating our access to their laboratory for hot pressing experiments. This work was supported by USDA funds through the Center for Wood Utilization at Oregon State University and by the Federal Ministry of Economics and Technology (Germany) through the German Wood Research Foundation (DGfH). The authors also acknowledge the encouragement of Drs. A. Fruehwald and A. Steffen.

References

Bodig J, Jayne BA (1982) Mechanics of wood and wood composites. Van Nostrand Reinhold Company, New York, p 712

Boehme C (1992) Die Bedeutung des Rohdichteprofils für MDF. Holz Roh- Werkst 50:18–24

Dai C, Knudson B, Wellwood R (2000) Research and Development in Oriented Strand Board (OSB) Processing. In: Proc. of the 5th Pacific Rim Bio-Based Composites Symposium, Canberra, pp 556–563

Fahrni F (1956) Das Verpressen von Spanplatten bei gefeuchteten oder feuchteren Deckspänen. Holz Roh- Werkst 14(1):8–10

von Haas G (1998) Untersuchungen zur Heißpressung von Holzwerkstoffmatten unter besonderer Berücksichtigung des Verdichtungsverhaltens, der Permeabilität, der Temperaturleitfähigkeit und der Sorptionsgeschwindigkeit. Dissertation, Univ. Hamburg, Germany, p 264

Haselein CR (1998) Numerical simulation of pressing wood-fiber composites. Ph.D. Thesis, Oregon State Univ., USA, p 244

Humphrey PE (1994) Engineering composites from oriented natural fibres: A strategy. In: Proc of the 2nd Pacific Rim Bio-Based Composites Symp., Vancouver, Canada, pp 2–8

Kehr E, Schölzel S (1965) Untersuchungen über das Preß-Diagramm zur Herstellung von Spanplatten. Drevarsky Vyskum 10(7):133–147

Kollmann F (1957) Über den Einfluß von Feuchtigkeitsunterschieden im Spangut vor dem Verpressen auf die Eigenschaften von Holzspanplatten. Holz Roh- Werkst 15(1):35–44

Kollmann F (1961) Rheologie und Strukturfestigkeit von Holz. Holz Roh- Werkst 19(7):73–80

Kull W (1963) Die Dichte von Holz und Holzwerkstoffen. Holz-Zentralblatt 89:125–131

Lang EM, Wolcott MP (1996) A model for visoelastic consolidation of wood-strand mats. Part II. Static stress-strain behavior of the mat. Wood Fiber Sci 28(7):369–379

Lenth CA, Kamke FA (1996) Investigations of flakeboard mat consolidation. Part II. Modeling mat consolidation using theories of cellular materials. Wood Fiber Sci 28(7):309–319

Liiri O (1969) Der Preßdruck bei der Spanplattenherstellung. Holz Roh- Werkst 27(8):371–378

May H-A, Mehlhorn L (1969) Verbesserung der Preßbedingungen durch die Anwendung von Regelsystemen anstelle von Programmsteuerungen. Holz-Zentralblatt 86:1342–1348

Pierce CB, Dinwoodie JM (1977) Creep in chipboard. Part I. Fitting 3- and 4-element response curves to creep data. J Mater Sci 12:1955–1960

Plath E (1971) Beitrag zur Mechanik der Holzspanplatten. Holz Roh- Werkst 29(8):377–382

Raczkowski J (1969) Der Einfluß von Feuchtigkeitsänderungen auf das Kriechverhalten des Holzes. Holz Roh- Werkst 27(6):232–237

Ren S (1991) Thermo-hygro rheological behavior of materials used in the manufacture of wood-based composites. Ph.D. Thesis, Oregon State Univ., USA, p 226

Steffen A, von Haas G, Rapp A, Humphrey PE, Thömen H (1999) Temperature and gas pressure in MDF-mats during industrial continuous hot pressing. Holz Roh- Werkst 57:154–155

Steiner PR, Dai C (1993) Spatial structure of wood composites in relation to processing and performance characteristics. Part I. Rationale and model development. Wood Sci Tech 28:45–51

Thoemen H (2000) Modeling the Physical Processes in Natural Fiber Composites During Batch and Continuous Pressing. Ph.D. Thesis, Oregon State Univ., USA, p 187

Thoemen H, Humphrey PE (2003) Modeling the continuous pressing process for wood-based composites. Wood Fiber Sci 35(7):456–468

Thoemen H, Humphrey PE (2005) Modeling the physical processes relevant during hot pressing of wood-based composites. Part I. Heat and mass transfer. (Submitted to Holz Roh- Werkst)

Wang S, Winistorfer PM, Moschler WW, Helton C (2000) Hot-pressing of oriented strandboard by step-closure. For Prod J 50(7):28–34

Winistorfer P, Moschler W, Wang S, DePaula E, Bledsoe BL (2000) Fundamentals of vertical density profile formation in wood composites. Part 1. In-situ density measurement of the consolidation process. Wood Fiber Sci 32(2):209–219

Zombori BG (2001) Modeling the transient effects during the hot-compression of wood-based composites. Ph.D. Thesis. Virginia State Univ., USA. p 212